

THE FAINT OPTICAL AFTERGLOW AND HOST GALAXY OF GRB 020124: IMPLICATIONS FOR THE NATURE OF DARK GAMMA-RAY BURSTS

E. BERGER¹, S. R. KULKARNI¹, J. S. BLOOM¹, P. A. PRICE^{1,2}, D. W. FOX¹, D. A. FRAIL^{1,3}, T. S. AXELROD², R. A. CHEVALIER⁴, E. COSTA⁵, S. G. DJORGOVSKI¹, F. FRONTERA^{6,7}, T. J. GALAMA¹, J. P. HALPERN⁸, F. A. HARRISON¹, J. HOLTZMAN⁹, K. HURLEY¹⁰, R. A. KIMBLE¹¹, P. J. MCCARTHY¹², L. PIRO⁵, D. REICHART¹, G. R. RICKER¹³, R. SARI¹⁴, B. P. SCHMIDT², J. C. WHEELER¹⁵, R. VANDERPPEK¹³
& S. A. YOST¹

Draft version June 22, 2019

ABSTRACT

We present ground-based optical observations of GRB 020124 starting 1.6 hours after the burst, as well as subsequent Very Large Array (VLA) and *Hubble Space Telescope* (HST) observations. The optical afterglow of GRB 020124 is one of the faintest afterglows detected to date, and it exhibits a relatively rapid decay, $F_\nu \propto t^{-1.60 \pm 0.04}$, followed by further steepening. In addition, a weak radio source was found coincident with the optical afterglow. The HST observations reveal that a positionally coincident host galaxy must be the faintest host to date, $R \gtrsim 29.5$ mag. The afterglow observations can be explained by several models requiring little or no extinction within the host galaxy, $A_V^{\text{host}} \approx 0 - 0.9$ mag. These observations have significant implications for the statistics of the so-called dark bursts (bursts for which no optical afterglow is detected), which are usually attributed to dust extinction within the host galaxy. The faintness and relatively rapid decay of the afterglow of GRB 020124, combined with the low inferred extinction indicate that some dark bursts are intrinsically dim and not dust obscured. Thus, the diversity in the underlying properties of optical afterglows must be observationally determined before substantive inferences can be drawn from the statistics of dark bursts.

Subject headings: gamma-rays:bursts — dust:extinction — cosmology:observations

1. INTRODUCTION

One of the main observational results stemming from five years of γ -ray burst (GRB) follow-ups at optical wavelengths is that about 60% of well-localized GRBs lack a detected optical afterglow, (“dark bursts”; Taylor et al. 2000; Fynbo et al. 2001; Reichart & Yost 2001; Lazzati, Covino, & Ghisellini 2002). In some cases, a non-detection of the optical afterglow could simply be due to a failure to image quickly and/or deeply enough. However, there are two GRBs for which there is strong evidence that the optical emission should have been detected, based on an extrapolation of the radio and X-ray emission (Djorgovski et al. 2001a; Piro et al. 2002). One interpretation in these two cases is that the optical light was extinguished by dust, either within the immediate environment of the burst or elsewhere along the line of sight (e.g. Groot et al. 1998). An alternative explanation is a high redshift, leading to absorption

of the optical light in the Ly α forest. However, the redshifts of the underlying host galaxies of these GRBs are of order unity (Djorgovski et al. 2001a; Piro et al. 2002).

Several authors have recently argued that a large fraction of the dark bursts are due to dust extinction within the local environment of the bursts (e.g. Reichart & Yost 2001; Lazzati et al. 2002; Reichart & Price 2002), but other scenarios have also been suggested (e.g. Lazzati et al. 2002). Moreover, it has been noted that regardless of the location of extinction within the host galaxy, the fraction of dark bursts is a useful upper limit on the fraction of obscured star formation (Kulkarni et al. 2000; Djorgovski et al. 2001b; Ramirez-Ruiz, Trentham, & Blain 2002; Reichart & Price 2002).

However, from an observational point of view, we must have a clear understanding of the diversity of afterglow properties before extracting astrophysically interesting inferences from dark

¹Division of Physics, Mathematics and Astronomy, 105-24, California Institute of Technology, Pasadena, CA 91125

²Research School of Astronomy & Astrophysics, Mount Stromlo Observatory, via Cotter Rd., Weston Creek 2611, Australia

³National Radio Astronomy Observatory, Socorro, NM 87801

⁴Department of Astronomy, University of Virginia, P.O. Box 3818, Charlottesville, VA 22903-0818

⁵Istituto Astrofisica Spaziale, C.N.R., Area di Tor Vergata, Via Fosso del Cavaliere 100, 00133 Roma, Italy

⁶Istituto Astrofisica Spaziale and Fisica Cosmica, C.N.R., Via Gobetti, 101, 40129 Bologna, Italy

⁷Physics Department, University of Ferrara, Via Paradiso, 12, 44100 Ferrara, Italy

⁸Columbia Astrophysics Laboratory, Columbia University, 550 West 120th Street, New York, NY 10027

⁹Department of Astronomy, MSC 4500, New Mexico State University, P.O. Box 30001, Las Cruces, NM 88003

¹⁰University of California at Berkeley, Space Sciences Laboratory, Berkeley, CA 94720-7450

¹¹Laboratory for Astronomy and Solar Physics, NASA Goddard Space Flight Center, Code 681, Greenbelt, MD 20771

¹²Carnegie Observatories, 813 Santa Barbara Street, Pasadena, CA 91101

¹³Center for Space Research, Massachusetts Institute of Technology, 70 Vassar Street, Cambridge, MA 02139-4307

¹⁴Theoretical Astrophysics 130-33, California Institute of Technology, Pasadena, CA 91125

¹⁵Astronomy Department, University of Texas, Austin, TX 78712

bursts. For example, afterglows which are faint or fade rapidly (relative to the detected population) would certainly bias the determination of the fraction of truly obscured bursts. In this vein, Fynbo et al. (2001), noting the faint optical afterglow of GRB 000630, argued that some dark bursts are due to a failure to image deeply and/or quickly enough, rather than dust extinction.

Here we present optical and radio observations of GRB 020124, an afterglow that would have been classified dark had it not been for rapid and deep searches. Furthermore, GRB 020124 is an example of an afterglow, which is dim due to the combination of intrinsic faintness and a relatively fast decline, and not strong extinction.

2. OBSERVATIONS

2.1. Ground-Based Observations

GRB 020124, localized by the HETE-II satellite on 2002, Jan 24.44531 UT, had a duration of ~ 70 s and a fluence ($6-400$ keV) of 3×10^{-6} erg cm $^{-2}$ (Ricker et al. 2002). Eight minutes after receiving the coordinates¹⁶ we observed the error box with the dual-band (B_M , R_M) MACHO imager mounted on the robotic 50-in telescope at the Mount Stromlo Observatory (MSO). We also observed the error box with the Wide-Field Imager on the 40-in telescope at Siding Spring Observatory (SSO). We were unable to identify a transient source within the large error box (Price, Schmidt, & Axelrod 2002).

We subsequently observed the error box refined by the Inter-Planetary Network (Hurley et al. 2002) with the Palomar 48-in Oschin Schmidt using the unfiltered NEAT imager. PSF-matched image subtraction (Alard 2000) between the MACHO and NEAT images revealed a fading source (Price et al. 2002), which was $R \approx 18$ mag at the epoch of our first observations, and not present in the Digitized Sky Survey. Two nights later we observed the afterglow using the Jacobs Camera (JCAM; Bloom et al. 2002b) mounted at the East arm focus of the Palomar 200-in telescope (Bloom et al. 2002a). The position of the fading source is $\alpha(J2000)=9^h32^m50.78^s$, $\delta(J2000)=-11^\circ31'10.6''$, with an uncertainty of about 0.4 arcsec in each coordinate (Fig. 1).

Using the Very Large Array (VLA¹⁷) we observed the fading source at 8.46 and 22.5 GHz (see Table 3). We detect a faint source, possibly fading, at 8.46 GHz located at $\alpha(J2000)=9^h32^m50.81^s$, $\delta(J2000)=-11^\circ31'10.6''$, with an uncertainty of about 0.1 arcsec in each coordinate. Given the positional coincidence between the fading optical source and radio detection we suggest this source to be the afterglow of GRB 020124.

The optical images were bias-subtracted and flat-fielded in the standard manner. To extract the photometry we weighted the aperture with a Gaussian equivalent to the seeing disk ("weighted-aperture photometry"), using IRAF/wphot. The photometric zero-points were set through photometry of calibrated field stars (Henden 2002) with magnitudes transformed to the appropriate system (Bessell & Germany 1999; Smith et al. 2002). The photometry is summarized in Tab. 1

2.2. Hubble Space Telescope Observations

We observed the afterglow with the *Hubble Space Telescope* (HST) using the Space Telescope Imaging Spectrograph (STIS) on 2002 Feb. 11.09, 18.30, and 25.71 UT (Bloom et al. 2002a), as part of our large HST Cycle 10 program (GO-9180, PI: Kulkarni). The HST observations consisted of 750–850 sec exposures. The HST data were retrieved after "On-The-Fly" pre-processing. Using IRAF we drizzled (Fruchter & Hook 2002) each image onto a grid with pixels smaller than the original by a factor of two and using `pixfrac` of 0.7.

We found an astrometric tie between the HST and JCAM images using IRAF/geomap with nine suitable astrometric tie objects in common between the images. The rms of the resultant mapping is 133 mas (RA) and 124 mas (Dec). Using this mapping and IRAF/geoxytrans we transferred the afterglow position on the JCAM image to the HST images. The rms of the transformation is 604 mas (RA) and 596 mas (Dec), and is dominated by the uncertainty in the JCAM position.

The source "S1" (Fig. 2) coincides with the afterglow position within the astrometric uncertainty. We performed differential photometry at the position of S1 by registering the images of epochs 1 and 2 using a cross-correlation of a field of size 10 arcsec centered on S1 (using IRAF/crosscor and shiftfind). We used IRAF/center and the FWHM of a relatively bright point source ("PSF star"; Fig. 1) to fix the position of S1 in each of the final images, and to determine the uncertainty in the position.

We photometered the source (and the PSF star) in epoch 1 using IRAF/phot, and determined a count-rate of 0.0921 ± 0.013 e $^-$ s $^{-1}$ (corrected by 17% for the loss of flux from an infinite aperture radius). Using IRAF/synphot and assuming a source spectrum of $f_\lambda \propto \lambda^{-1.4}$ (see below), we find that the source was $R = 28.55^{+0.16}_{-0.14}$ mag at the time of epoch 1. The photometry of the three epochs is summarized in Tab. 2. Please note that this more careful analysis supersedes our preliminary report (Bloom et al. 2002c).

There are no obvious persistent sources within 1.75 arcsec of the OT down to $R \approx 29.5$ mag. To date, all of the GRBs localized to sub-arcsecond accuracy have viable hosts brighter than this level within ~ 1.3 arcsec of the OT position (Bloom, Kulkarni, & Djorgovski 2002). The faintest host to date is that of GRB 990510, $R \sim 28.5$ mag ($z=1.619$; Vreeswijk et al. 2001). Thus, the host of GRB 020124 may be at a somewhat higher redshift; however, $z \lesssim 4.5$ since the afterglow was detected in the B_M filter.

3. MODELING OF THE OPTICAL DATA

In Figure 3 we plot the optical lightcurves of GRB 020124, including a correction for Galactic extinction, $E(B-V) = 0.052$ mag (Schlegel et al. 1998). The optical lightcurves are usually modeled as $F_\nu(t, \nu) = F_{\nu,0}(t/t_0)^\alpha(\nu/\nu_0)^\beta$. However, as can be seen in Fig. 3, the R -band lightcurve cannot be described by a single power law. Restricting the fit to $t < 2$ days we obtain ($\chi^2_{\min} = 15$ for 14 degrees of freedom) $\alpha_1 = -1.60 \pm 0.04$, $\beta = -1.43 \pm 0.14$, and $F_{\nu,0} = 2.96 \pm 0.25$ μ Jy; here $F_{\nu,0}$ is defined at the effective frequency of the R_M filter and $t = 1$ day. For $t > 2$ days we get $\alpha_2 \approx -1.9$.

To account for the steepening we modify the model for the

¹⁶This corresponds to 1.6 hours after the burst detection.

¹⁷The VLA is operated by the National Radio Astronomy Observatory, a facility of the National Science Foundation operated under cooperative agreement by Associated Universities, Inc.

R -band lightcurve to:

$$F_\nu(t, \nu) = F_{\nu,0}(\nu/\nu_0)^\beta [(t/t_b)^{\alpha_1 n} + (t/t_b)^{\alpha_2 n}]^{1/n}, \quad (1)$$

where, α_1 is the asymptotic index for $t \ll t_b$, α_2 is the asymptotic index for $t \gg t_b$, $n < 0$ provides a smooth joining of the two asymptotic segments, and t_b is the time at which the asymptotic segments intersect. We retain the simple model for the R_M and B_M lightcurves since they are restricted to $t \lesssim 0.13$ days (i.e. well before the observed steepening).

We investigate two alternatives for the observed steepening in the framework of the afterglow synchrotron model (e.g. Sari, Piran, & Narayan 1998). In this framework, α_1 , α_2 , and β are related to each other through the index (p) of the electron energy distribution, $N(\gamma) \propto \gamma^{-p}$ (for $\gamma > \gamma_{\min}$). The relations for the models discussed below, as well as the resulting closure relations, $\alpha_1 + \beta + c = 0$, are summarized in Tab. 4.

3.1. Cooling Break

The observed steepening, $\Delta\alpha \equiv \alpha_2 - \alpha_1 \approx -0.3$, can be due to the passage of the synchrotron cooling frequency, ν_c , through the R -band. This has been inferred, for example, in the afterglow of GRB 971214, at $t \sim 0.2$ days (Wijers & Galama 1999). If the steepening is due to ν_c , this rules out models in which the ejecta expand into a circumburst medium with $\rho \propto r^{-2}$ (hereafter, Wind), because in this model ν_c increases with time ($\propto t^{1/2}$; Chevalier & Li 1999), and one expects $\Delta\alpha = 0.25$.

There are two remaining models to consider in this case: (i) spherical expansion into a circumburst medium with constant density (hereafter, ISM_B; Sari, Piran, & Narayan 1998), and (ii) a jet with $\theta_{\text{jet}} < \Gamma_{t \sim 0.06 \text{ d}}^{-1}$ (i.e. a jet break prior to the first observation at $t \approx 0.06$ days; hereafter, Jet_B). The subscript B indicates that ν_c is blueward of the optical bands initially. In both models we use Eqn. 1 for the R -band lightcurve, with t_b defined as the time at which $\nu_c = \nu_R$, and $\alpha_2 \equiv \alpha_1 - 1/4$.

We find that in the ISM_B model $t_c \approx 0.4$ days, while in the Jet_B model $t_c \approx 0.65$ days. Moreover, in both models the closure relations can only be satisfied by including a contribution from dust extinction within the host galaxy, A_V^{host} . We estimate the required extinction using the parametric extinction curves of Cardelli, Clayton, & Mathis (1989) and Fitzpatrick & Massa (1988), along with the interpolation calculated by Reichart (2001). Since the redshift of GRB 020124 is not known we assume $z = 0.3, 1, 3$, which spans the range of typical redshifts for the long-duration GRBs. The inferred values of A_V^{host} are summarized in Tab. 4, and range from 0.2 to 0.9 mag.

3.2. Jet Break

An alternative explanation for the steepening is a jet expanding into: (i) an ISM medium with ν_c blueward of the optical bands (J-ISM_B), (ii) a Wind medium with ν_c blueward of the optical bands (J-Wind_B), and (iii) an ISM or Wind medium with ν_c redward of the optical bands (J-ISM/Wind_R). We note that the J-ISM_B model is different than the ISM_B model (§3.1) since previously it was defined such that the jet break is later than the last observation. In these models, $t_b \equiv t_{\text{jet}}$ is the time at which $\Gamma(t_{\text{jet}}) \approx \theta_{\text{jet}}^{-1}$.

From the closure values we note that the J-ISM/Wind_R requires no extinction within the host galaxy, while the J-ISM_B and J-Wind_B models require values of about 0.05 to 0.3 mag.

We find $t_{\text{jet}} \sim 10$ –20 days, corresponding to $\theta_{\text{jet}} \sim 10^\circ$. Using the measured fluence (§2.1) we estimate the beaming-corrected γ -ray energy, $E_\gamma \approx 5 \times 10^{50}$ erg, assuming a circumburst density of 1 cm^{-3} and $z = 1$ (E_γ is a weak function of z). This value is in good agreement with the distribution of E_γ for long-duration GRBs (Frail et al. 2001).

4. DISCUSSION AND CONCLUSIONS

Regardless of the specific model for the afterglow emission, the main conclusion of §3 is that the optical afterglow of GRB 020124 suffered little or no dust extinction. Still, this afterglow would have been missed by typical searches undertaken even as early as 12 hours after the GRB event. As shown in Fig. 4, about 70% of the searches conducted to date would have failed to detect an optical afterglow like that of GRB 020124.

This is simply because the afterglow of GRB 020124 was faint and exhibited relatively rapid decay. From Fig. 5 we note that GRB 020124 is one of the faintest afterglows detected to date (normalized to $t = 1$ day), and while it is not an excessively rapid fader, it is in the top 30% in this category.

Thus, the afterglow of GRB 020124, along with that of GRB 000630 (Fynbo et al. 2001; Fig. 5), indicates that there is a wide diversity in the brightness and decay rates of optical afterglows. In fact, the brightness distribution spans a factor of about 400, while the decay index varies by more than a factor of three. Coupled with the low dust extinction in the afterglow of GRB 020124, this indicates that some dark bursts may simply be dim, and not dust obscured.

Given this wide diversity in the brightness of optical afterglows, it is important to establish directly that an afterglow is dust obscured. This has only been done in a few cases (§1). Therefore, while *statistical* analyses (e.g. Reichart & Yost 2001) point to extinction as the underlying reason for some fraction of dark bursts, and may even account for an afterglow like that of GRB 020124, it is clear that observationally the issue of dark bursts is not settled, and the observational biases have not been traced fully.

Since progress in our understanding of dark bursts will benefit from observations, we need consistent, rapid follow-up of a large number of bursts to constrain the underlying distribution, as well as complementary techniques which can directly measure material along the line of sight. This includes X-ray observations which allow us to measure the column density to the burst (Galama & Wijers 2001), and thus infer the type of environment, and potential extinction level. Along the same line, radio observations allow us to infer the synchrotron self-absorption frequency, which is sensitive to the ambient density (e.g. Sari & Esin 2001); the detection of radio emission, as in the case of GRB 020124, implies a density $n \lesssim 10^2 \text{ cm}^{-3}$. Finally, prompt optical observations, as we have carried out in this case, may uncover a larger fraction of the dim optical afterglows, and provide a better constraint on the fraction of truly obscured bursts.

J. S. B. is a Fannie and John Hertz Foundation Fellow. F. A. H. acknowledges support from a Presidential Early Career award. S. R. K. and S. G. D. thank the NSF for support. R. S. is grateful for support from a NASA ATP grant. R. S. and T. J. G. acknowledge support from the Sherman Fairchild Foundation. J. C. W. acknowledges support from NASA grant

NAG59302. K. H. is grateful for Ulysses support under JPL contract 958056 and for IPN support under NASA grants FD-NAG 5-11451 and NAG 5-17100. Support for Proposal HST-GO-09180.01-A was provided by NASA through a grant from

the Space Telescope Science Institute, which is operated by the Association of Universities for Research in Astronomy, Inc., under NASA contract NAS5-26555.

REFERENCES

- Alard, C. 2000, *A&AS*, 144, 363.
 Bessel, M. S., & Germany, L. M. 1999, *PASP*, 111, 1421.
 Bloom, J. S. 2002a, GCN 1225.
 Bloom, J. S., et al. 2002b, Submitted to *PASP*.
 Bloom, J. S., et al. 2002c, GCN 1389.
 Bloom, J. S., Kulkarni, S. R., & Djorgovski, S. G. 2002, *AJ*, 123, 1111.
 Cardelli, J. A., Clayton, G. C., & Mathis, J. S. 1989, *ApJ*, 345, 245.
 Castro-Tirado, A. J., et al. 2001, *A&A*, 370, 398.
 Chevalier, R. A., & Li, Z.-Y. 1999, *ApJ*, 520, L29.
 Djorgovski, S. G., et al. 2001a, *ApJ*, 562, 654.
 Djorgovski, S. G., et al. 2001b, in *Proc. Gamma-ray Bursts in the Afterglow Era: 2nd Workshop*, ed. N. Masetti et al., *ESO Astrophysics Symposia*, Berlin: Springer Verlag, 218.
 Esin, A. A., & Blandford, R. 2000, *ApJ*, 534, L151.
 Fitzpatrick, E. L., & Massa, D. 1988, *ApJ*, 328, 734.
 Frail, D. A., et al. 2001, *ApJ*, 562, L55.
 Fruchter, A. S., & Hook, R. N. 2002, *PASP*, 114, 144.
 Fynbo, J. U., et al. 2001, *A&A*, 369, 373.
 Galama, T. J., & Wijers, R. A. M. J. 2001, *ApJ*, 549, L209.
 Gorosabel, J., et al. 2002, GCN 1224.
 Groot, P. J., et al. 1998, *ApJ*, 502, L123.
 Henden, A. 2002, GCN 1251.
 Hurley, K. H., et al. 2002, GCN 1223.
 Kulkarni, S. R., et al. 2000, in *Proc. SPIE Discoveries and Research Prospects from 8- to 10-Meter-Class Telescopes*, ed. J. Bergeron, 4005, 9.
 Lazzati, D., Covino, S., & Ghisellini, G. 2002, *MNRAS*, 330, 583.
 Piro, L., et al. 2002, *ApJ* in press; astro-ph/0201282.
 Price, P. A., Schmidt, B. P., & Axelrod, T. S. 2002, GCN 1219.
 Price, P. A., et al. 2002, GCN 1221.
 Ramirez-Ruiz, E., Trentham, N., & Blain, A. W. 2002, *MNRAS*, 329, 465.
 Reichart, D. E. 2001, *ApJ*, 553, 235.
 Reichart, D. E., & Yost, S. 2001, Submitted to *ApJ*; astro-ph/0107545.
 Reichart, D. E., & Price, P. A. 2002, *ApJ*, 565, 174.
 Rhoads, J. E., 1997, *ApJ*, 478, L1.
 Ricker, G., et al. 2002, GCN 1220.
 Sari, R., Piran, T., & Narayan, R. 1998, *ApJ*, 497, L17.
 Sari, R., Piran, T., & Halpern, J. P. 1999, *ApJ*, 519, L17.
 Sari, R., & Esin, A. A. 2001, *ApJ*, 548, 787.
 Schlegel, D., et al. 1998, *ApJ*, 500, 525.
 Smith, J. A., et al. 2002, *AJ* in press; astro-ph/0201143.
 Taylor, G. B., et al. 2000, *ApJ*, 537, L17.
 Vreeswijk, P. M., et al. 2001, *ApJ*, 546, 672.
 Waxman, E., & Draine, B. T. 2000, *ApJ*, 537, 796.
 Wijers, R. A. M. J., & Galama, T. J. 1999, *ApJ*, 523, 177.

TABLE 1
GROUND-BASED OPTICAL OBSERVATIONS OF GRB 020124

UT	Telescope	Band	Magnitude
Jan 24.51204	MSO 50	R_M	17.918 ± 0.041
Jan 24.51204	MSO 50	B_M	18.628 ± 0.057
Jan 24.51516	SSO 40	R	18.219 ± 0.046
Jan 24.51655	MSO 50	R_M	17.984 ± 0.044
Jan 24.51655	MSO 50	B_M	18.727 ± 0.063
Jan 24.51938	SSO 40	R	18.371 ± 0.091
Jan 24.52106	MSO 50	R_M	18.111 ± 0.049
Jan 24.52106	MSO 50	B_M	18.842 ± 0.069
Jan 24.52373	SSO 40	R	18.376 ± 0.082
Jan 24.55791	MSO 50	R_M	18.678 ± 0.048
Jan 24.55791	MSO 50	B_M	19.661 ± 0.090
Jan 24.56243	MSO 50	R_M	18.867 ± 0.036
Jan 24.56243	MSO 50	B_M	19.584 ± 0.053
Jan 24.56696	MSO 50	R_M	18.843 ± 0.039
Jan 24.56696	MSO 50	B_M	19.714 ± 0.050
Jan 26.34100	P 200	r'	24.398 ± 0.228

NOTE.—The columns are (left to right), (1) UT date of each observation, (2) telescope (MSO 50: Mt. Stromlo Observatory 50-in; SSO 40: Siding Spring Observatory 40-in; P 200: Palomar Observatory 200-in), (3) observing band, and (4) magnitudes and uncertainties. The observed magnitudes are not corrected for Galactic extinction.

TABLE 2
HST/STIS OBSERVATIONS OF GRB 020124

Epoch (UT)	Band	Exp. Time (ksec)	Flux ($\text{e}^- \text{s}^{-1}$)	S/N	Magnitude
Feb 11.09	50 CCD/Clear	10.0	0.0814 ± 0.0169	4.82	$R = 28.68^{+0.25}_{-0.20}$
Feb 18.30	50 CCD/Clear	7.4	0.0443 ± 0.0189	2.34	$R = 29.35^{+0.60}_{-0.39}$
Feb 25.71	50 CCD/Clear	7.5	0.0362 ± 0.0183	1.98	$R = 29.56^{+0.76}_{-0.44}$
Feb 18.30+25.71	50 CCD/Clear	14.9	0.0398 ± 0.0137	2.91	$R = 29.46^{+0.46}_{-0.32}$

NOTE.—The columns are (left to right), (1) UT date of each observation, (2) STIS CCD mode, (3) exposure time, (4) flux and uncertainty, (5) significance, and (6) R magnitude and uncertainty. The total number of counts was converted to the R -band assuming the observed color of the OT, $f_\lambda \propto \lambda^{-0.4}$ (§2.2). For epochs 2 and 3, the 3σ upper limits are: $R = 29.09$ and $R = 29.13$ mag, respectively. The observed magnitudes are not corrected for Galactic extinction.

TABLE 3
VLA RADIO OBSERVATIONS OF GRB 020124

Epoch (UT)	ν_0 (GHz)	Flux Density (μ Jy)
Jan 26.22	8.46	84 ± 30
Jan 26.25	22.5	-60 ± 100
Jan 27.22	8.46	45 ± 25
Feb 1.40	8.46	49 ± 17
Jan 26.22-Feb 1.40	8.46	48 ± 13

NOTE.—The columns are (left to right), (1) UT date of each observation, (2) observing frequency, and (3) flux density at the position of the radio transient with the rms noise calculated from each image. The last row gives the flux density at 8.46 GHz from the co-added map.

TABLE 4
AFTERGLOW MODELS

Model	α_1	α_2	β	(b, c)	Closure	p	A_V^{host} (mag)
ISM _B	$-\frac{3(p-1)}{4}$	$-\frac{3p}{4} + \frac{1}{2}$	$-\frac{p-1}{2}$	$(-3/2, 0)$	0.52 ± 0.28	3.17 ± 0.05	(0.35, 0.18, 0.10)
Jet _B	$-p$	$-p$	$-\frac{p-1}{2}$	$(-2, 1)$	2.23 ± 0.36	1.63 ± 0.04	(0.89, 0.50, 0.22)
J-ISM _B	$-\frac{3(p-1)}{4}$	$-p$	$-\frac{p-1}{2}$	$(-3/2, 0)$	0.52 ± 0.28	3.17 ± 0.05	(0.30, 0.10, 0.05)
J-Wind _B	$-\frac{3p-1}{4}$	$-p$	$-\frac{p-1}{2}$	$(-3/2, 1/2)$	1.02 ± 0.28	2.51 ± 0.05	(0.30, 0.16, 0.08)
J-ISM/Wind _R	$-\frac{3p-2}{4}$	$-p$	$-\frac{p}{2}$	$(-3/2, -1/2)$	0.02 ± 0.28	2.84 ± 0.05	...

NOTE.—The columns are (left to right), (1) Afterglow model (ISM: r^0 circumburst medium; Wind: r^{-2} circumburst medium; Jet: collimated eject with opening angle θ_{jet} ; a subscript *B* indicates $\nu_c < \nu_{\text{opt}}$, and a subscript *R* indicates $\nu_c > \nu_{\text{opt}}$), (2) α_1 as a function of p , (3) α_2 as a function of p , (4) β as a function of p , (5) closure relations ($\alpha + b\beta + c = 0$), (6) resulting closure values from the observed values of α_1 and β , (7) inferred value of p from the measured value of α_1 , and (8) the required extinction in the frame of the host galaxy for closure values of zero ($z = 0.3, 1, 3$); typical uncertainties are ± 0.05 mag. The top two models apply to the case when the observed steepening in the lightcurves is due to the passage of ν_c through the *R*-band, while the bottom three apply to the case when the steepening is due to a jet.

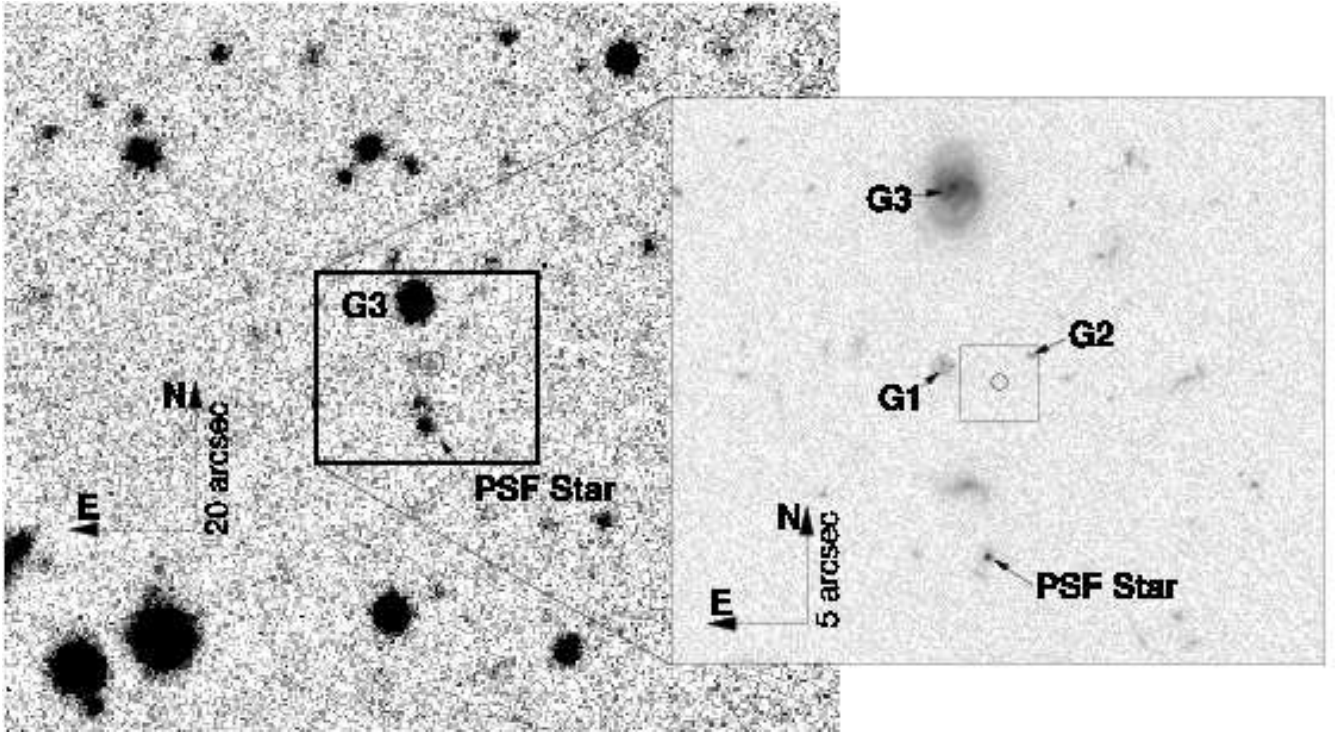


FIG. 1.— Palomar 200-inch (left) and HST epoch 1 (inset) images of the field of GRB 020124. The OT is circled in both images. The OT was of comparable brightness to G1 at the epoch of the P 200 image and significantly fainter than G1 three weeks later. The box overlaying the inset shows the portion of the HST images depicted in Figure 2. Relevant sources described in the text are noted. The HST image is shown with logarithmic scaling to highlight the features of nearby galaxies..

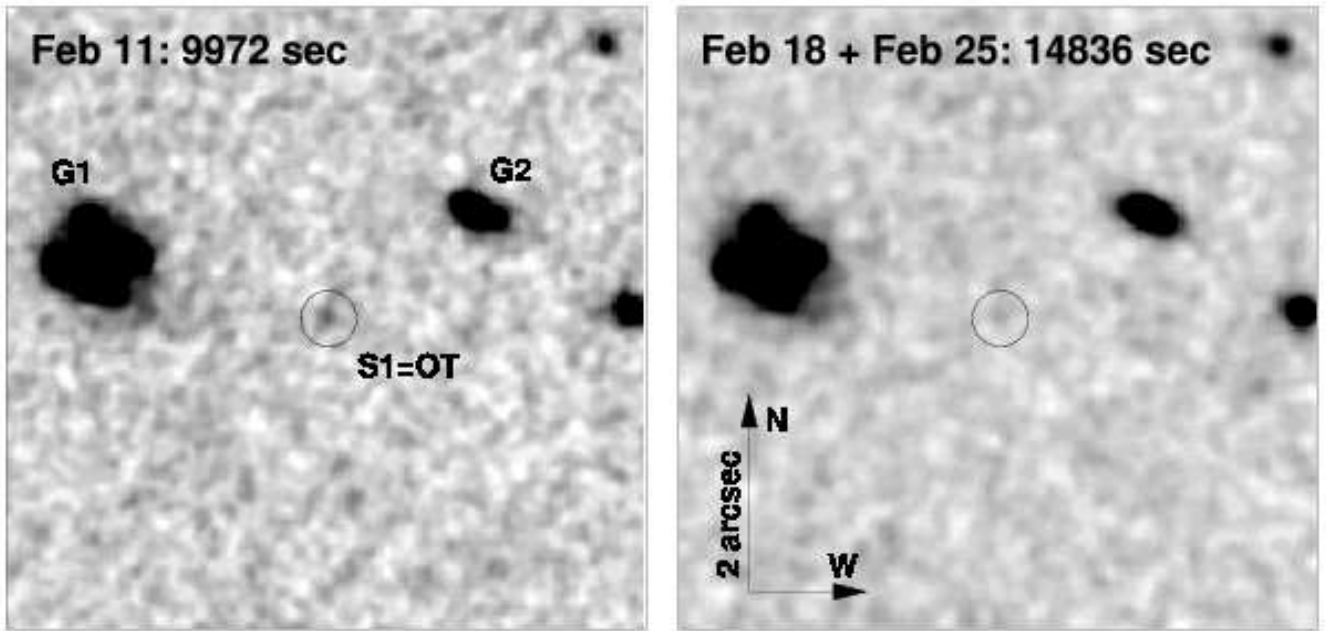


FIG. 2.— The faint optical transient (OT) of GRB 020124 as viewed using HST/STIS. Shown are the summed, smoothed images from epoch 1 (left) and epochs 2+3 (right). The greyscales have been matched such that a given flux is represented by the same shade in each image. The circle is centered at the same sky position in both images. Clearly, the source S1, identified with the position of the afterglow of GRB 020124 has faded.

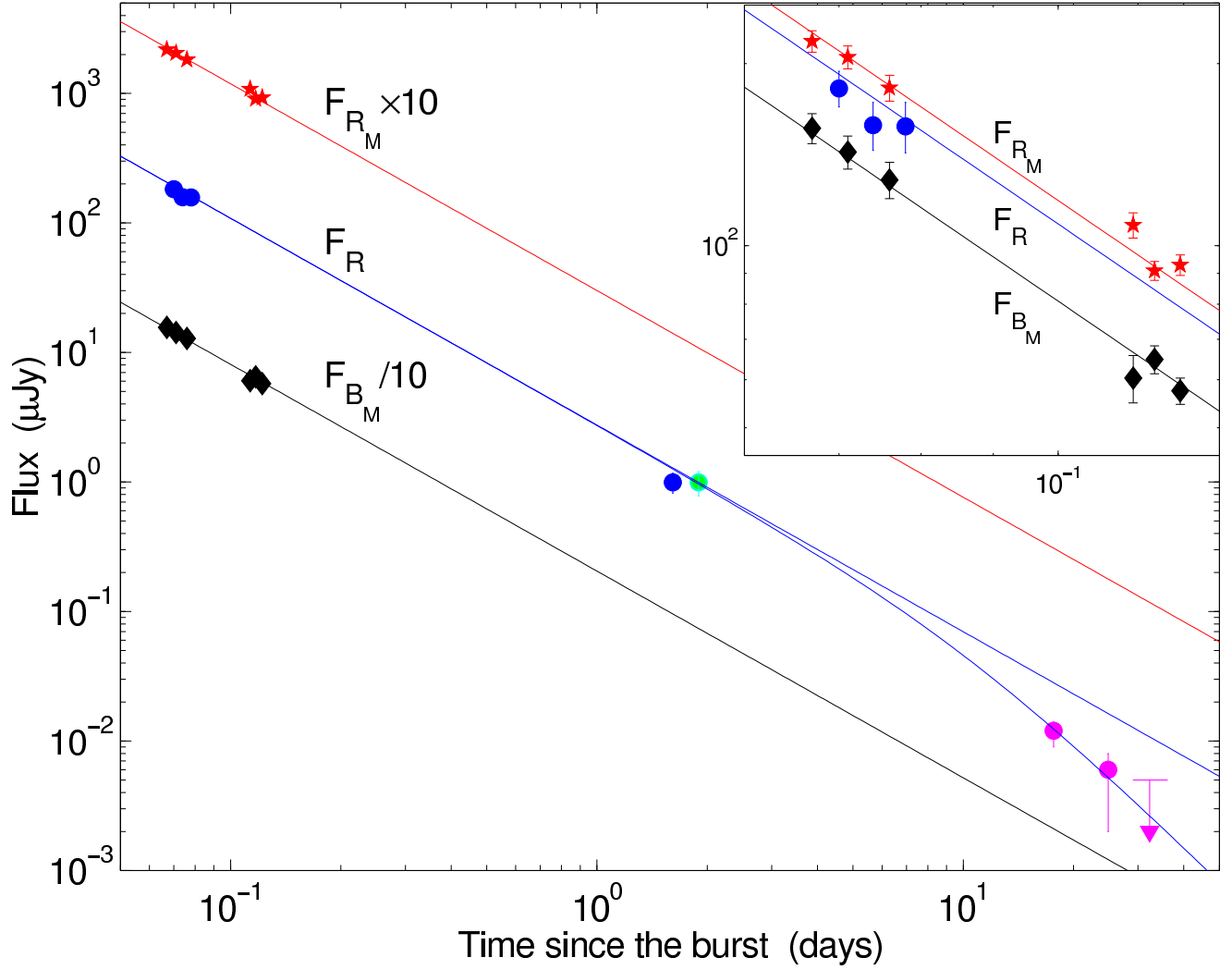


FIG. 3.— Optical lightcurves of GRB 020124 (top to bottom: R_M , R , and B_M), corrected for Galactic extinction, $E(B-V) = 0.052$ mag (Schlegel et al. 1998). The solid lines are a representative jet model (ISM/Wind_R; see Tab. 4), while the dashed line is an extrapolation of the early evolution without a break. With no break in the R -band lightcurve, the predicted magnitude at the epoch of the first HST observation exceeds the measured values by 5σ . The flux measured in the last HST epoch is plotted as a 2σ upper limit.

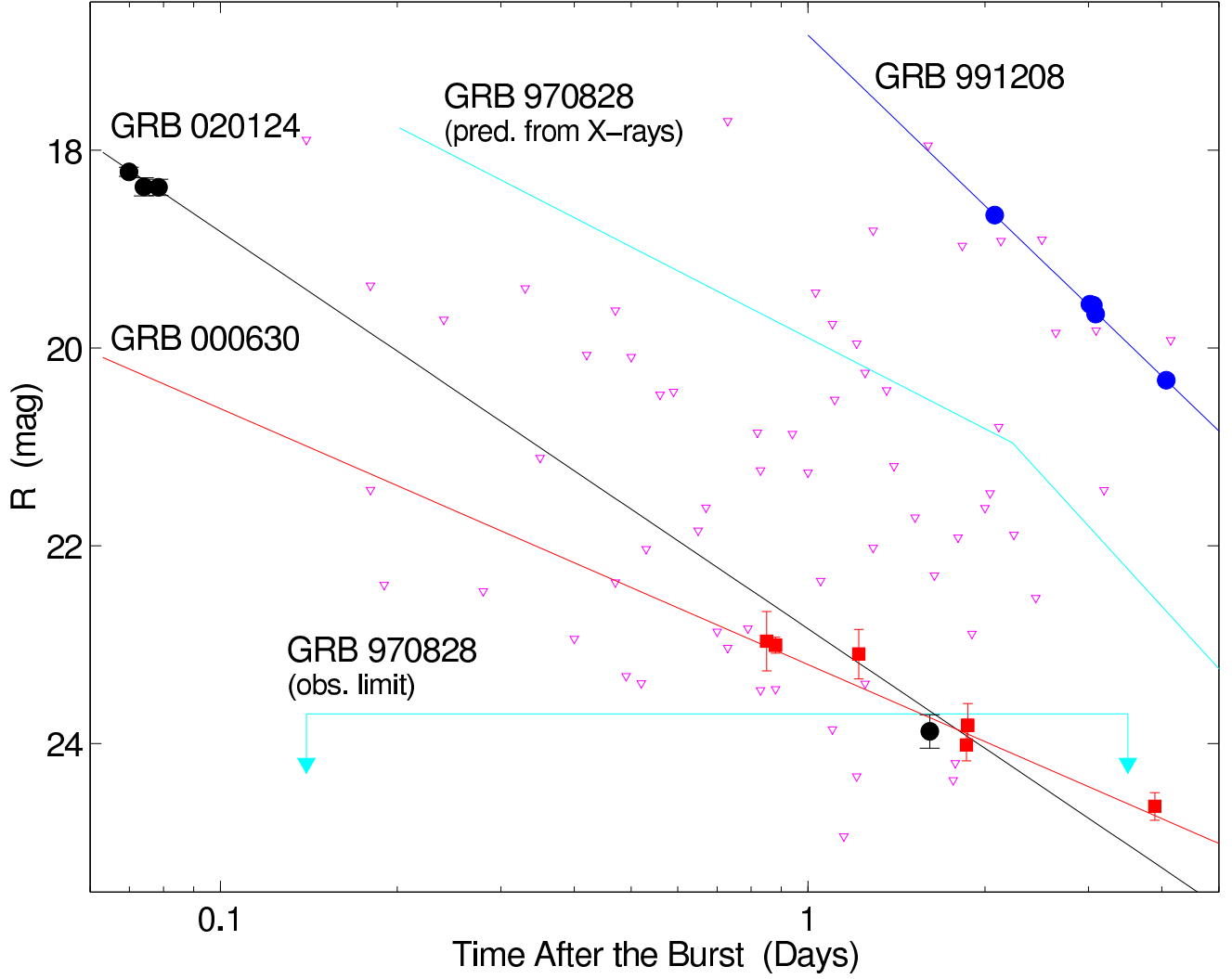


FIG. 4.— *R*-band upper limits from searches of well-localized GRBs, corrected for Galactic extinction. The limits up to GRB 000630 are taken from Fynbo et al. (2001), while subsequent limits are from the GRB Coordinates Network. Also shown are the lightcurves of the GRB 020124, GRB 000630, the bright GRB 991208 (Castro-Tirado et al. 2001), and GRB 970828 (the de-reddened lightcurve is based on the radio and X-ray data; Djorgovski et al. 2001). Only about 30% of the searches yielded limits that are fainter than the afterglow of GRB 020124. A similar fraction was found by Fynbo et al. (2001) based on the afterglow of GRB 000630.

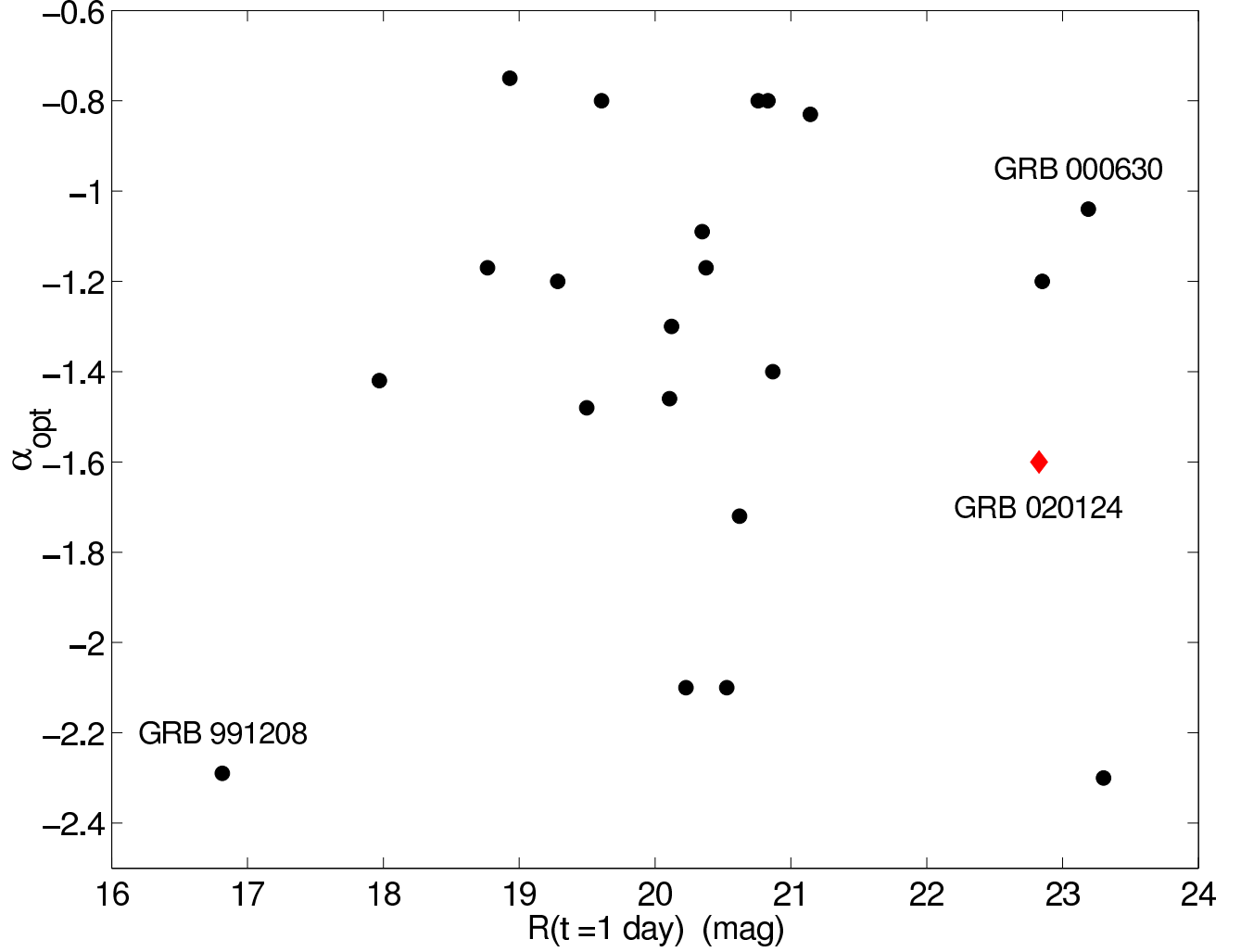


FIG. 5.— Temporal decay index, α_{opt} ($F_{\nu} \propto t^{\alpha}$), plotted against the R -band magnitude at $t = 1$ day for several optical afterglows. We chose a fiducial time of 1 day since, with the exception of GRB 010222, all the observations are before the jet break. While the majority of optical afterglows cluster around $R(t = 1 \text{ d}) \sim 20$ mag, GRB 020124 is one of the four faintest afterglows detected to date, and one of the six most rapid faders.